Speed Control for Multi-Three Phase Synchronous Electrical Motors in Fault Condition

Alessandro Galassini, Alessandro Costabeber, Chris Gerada
Power Electronic Machine Control Group (PEMC), The University of Nottingham, UK

***Abstract*—The growth of electrification transportation systems is an opportunity for delving into new feasible solutions for more reliable and fault tolerant arrangements. So far, many investigations distant from the market have been carried out. Most of the works are looking at new control strategies adding extra components increasing manufacturing efforts and costs. Considering a nine phase synchronous multi-three phase electrical motor with disconnected neutral points, this manuscript compares the common speed reference configuration (where all the drives are configured in speed mode) and the torque follower configuration (where one drive is in speed mode and all the others are in torque mode). Furthermore, a post-fault operation in open-circuit condition is proposed. Analytical equations and experimental validation in nominal and fault condition are given by means of Matlab/Simulink simulations and by experimental on a 22kW test rig.**

***Index Terms*—Common speed reference, Torque follower, Speed control, Multi-three phase, drives**

I. Introduction

Nowadays, in a market where three-phase electrical motors are predominant, the Two-Level three-phase Voltage Source Inverter (2L-3P-VSI) shown in Fig. 1 is the "de facto" off-the-shelf power converter topology for variable-speed AC drives [1]. Electrification transportation systems is pushing the boundaries in terms of operating ranges, performances and reliability on both machine and power converter side. When off-the-shelf technologies are not enough for input design specifications or when a certain system reliability level cannot be achieved, multi-three phase arrangements are one of the most attractive solutions [2]. Recently, several studies on multi-three phase electrical motors have been carried on by both industry and academia [3], and so far, multi-three phase degrees of freedom have been exploited for very different challenging applications from higher power generators to very small and integrated motors [3]–[6]. Combining different multi-phase machines to different power converters, many and very diverse arrangements and control strategies can be achieved and new sensor-less techniques can be developed [7].

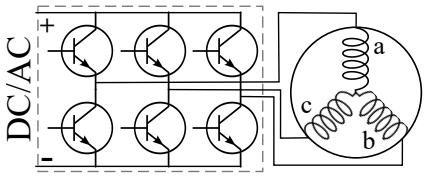

Fig. 1. Two-Level three-phase Voltage Source Inverter (2L-3P-VSI) and one three phase set of windings (a, b, c).

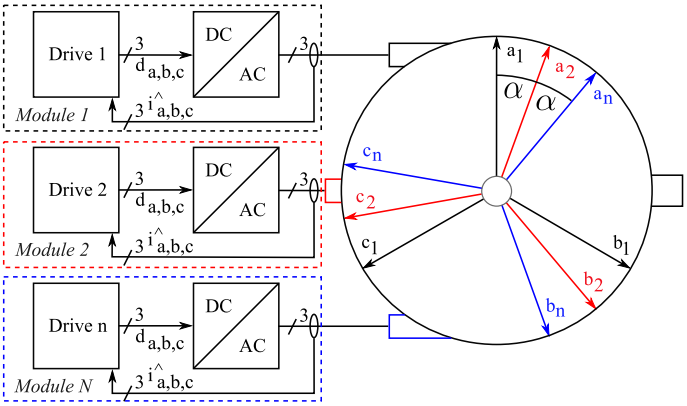

Fig. 2. Nine phase ($n = 9$) multi-three phase machine with disconnected neutral points wired to three ($N = 3$) 2L-3P-VSI (DC/AC blocks). Current feedbacks ($i_a^{\wedge}$,$i_b^{\wedge}$,$i_c^{\wedge}$) are routed to each local drive. d_a,d_b,d_c = duty cycles.

In this work, a comparison between two speed-controlled industrial multi-drive arrangements applied to a triple-star synchronous machine with disconnected neutral points (Fig. 2) is provided by mean of Matlab/Simulink simulations and by experimental on a $22kW$ test rig. Control design in nominal condition and post-fault operation for constant speed dynamics with one set of windings in open-circuit are presented.

Routing the three local current signals only to their relative drive allows costs to be contained. Large scale market economy and redundancy are achieved connecting a 2L-3P-VSI per three-phase set of windings. In-fact, the arrangement in Fig. 2 can be split into different independent modules (or segment) with one drive (or micro-controller), one 2L-3P-VSI, and one set of windings.

In the next section, multi-drive configurations are introduced and differences between industrial multi-drive arrangements and the proposed multi-three phase arrangement are discussed. In Sec. III, modelling assumption for both machine and drives are given. A simplified design approach is introduced in Sec. IV, and it is further extended to the open-circuit fault condition in Sec. V. After presenting a case study in Sec. VI, the validation of the proposed analysis is provided in Sec. VII.

II. Multi-drive configurations

Usually, in order to achieve better current dynamics, multi-three phase arrangements based on the so called Vector Space Decomposition (VSD) [8] are centralised like in Fig. 4. All current feedbacks are provided to the only drive within the system. The same drive sets all the duty cycles for all the

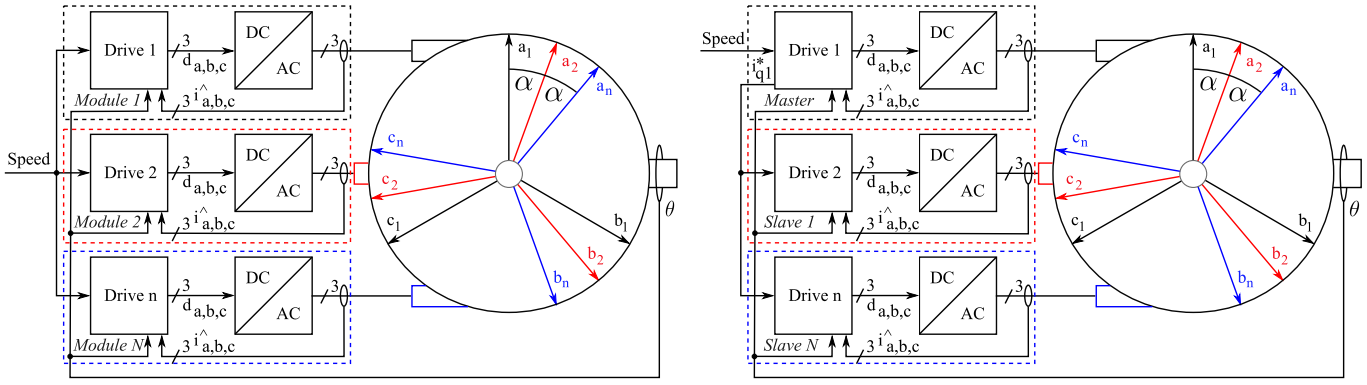

(a) Common Speed Reference configuration (CSR). (b) Torque Follower configuration (TF).

Fig. 3. Whilst the CSR is distributed, the TF is centralised. In the TF, the master-drive internal current set-point i^*_{q1} within the reference frame is provided as input to the slave-drives. In both the configurations every drive processes only its local current feedbacks. θ is the mechanical angle. $\alpha = \pi/n$.

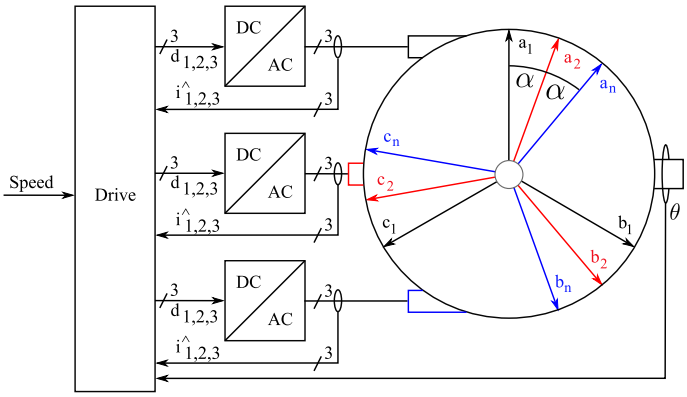

Fig. 4. Centralised configuration with one single drive processing all the current feedbacks.

converters. Despite the system in Fig. 4 allows new control strategies to be studied [9], it is not redundant on the drive side. On the other hands, having one drive per converter, both configurations in Fig. 3 are fully redundant. Furthermore, *know-how* on three-phase vector-control theory and fault management [10] can be re-used, and eventually combined for developing new control strategies [11] and post-fault countermeasures [12], [13].

Multi-drive systems are very common in industrial plants (i.e. conveyor belts, conveying lines with a common line shaft or large bull gears with multiple driven motors). In application notes for AC variable-speed drive with load sharing capabilities [14], the Common Speed Reference (CSR) configuration in Fig. 3a is advised with non-rigid loads (i.e. conveyor belts). Contrarily, the Torque follower (TF) configuration in Fig. 3b is suggested with rigid mechanical coupling (i.e. bull gears). The CSR (Fig.3a) presents all the drives configured in speed mode. Being all the drives the same, the CSR configuration is distributed. On the other hands, the TF one (Fig.3b) is based on a master/slave approach, where the master-drive is in speed mode and the slaves are in torque mode. Provided that input for the slave-drives is the internal current set-point of the master-drive, the TF configuration is centralised and in case of master-drive fault, the system is compromised. For sake of completeness, another load sharing technique in between the CSR and of TF configuration called speed-trim follower (STF) configuration is listed. The STF can be adopted when the coupling among motors has a very high potential for oscillation. Since not distributed and in between the CSR and the TF configuration, it will not be discussed in this work. Such a kind of application notes were written for completely independent variable-speed off-the-shelf AC drives wired to different three-phase off-the-shelf motors coupled together. In multi-drive industrial plants, the coupling among different motors, either rigid or not, is not ideal. In-fact, even if in small extent, oscillations and skews are always present [15]. Contrarily, in multi-three phase motors the rotor position information (θ in Fig. 3) is common to all the drives. Since there is just one rotor electro-magnetically coupled to multiple sets of windings, the resulting mechanical coupling among the drives can be considered ideal. For this reason, as it will be later shown, in multi-three phase motors there is no difference between the CSR and the TF configuration.

III. Modelling

Multi-three phase electrical motors are a particular group of split-phase winding machines. Defining m the number of phases per set of windings $m = 3$. Defining N the number of sets of windings, the total number of phases is equal to $n = Nm$. The motor modelled in this paper and shown in Fig. 2-4 is composed by nine phases ($m = 3$, $N = 3$, $n = 9$) and with phase progression $\alpha = \pi/n$.

A. Machine modelling assumptions

The work presented in this paper is based on the assumption that stator inductances are constant. Therefore, it applies to electric machines with negligible saturation effects. In addition it is assumed that:

- all phases are geometrically identical;
- each phase is symmetrical around its magnetic axis;

- the spatial displacement between two whatever phases is an integer multiple of the phase progression α;
- within the air-gap, only the fundamental component of magneto-motive force is considered.

No restrictive assumption is made, instead, about whether the winding is distributed or concentrated and no leakage flux component is ignored [16], [17].

Three-phase machine stator variables (i.e. voltage, current, etc., denoted with subscript abc) can be transformed within the rotor-attached orthogonal $dq0$ reference frame (denoted with subscript dq) thanks to the Park's transformation [18]. Distributed current control of the machine can be achieved thanks to the following equation [19]:

$$\mathbf{v}_{dq} = \mathbf{R}_{dq}\mathbf{i}_{dq} + \mathbf{L}_{dq}\frac{d\mathbf{i}_{dq}}{dt} \tag{1}$$

where $\mathbf{v}_{dq}$ and $\mathbf{i}_{dq}$ are voltage and current vectors $nx1$, respectively. $\mathbf{R}_{dq}$ and $\mathbf{L}_{dq}$ are resistance and inductance matrices nxn, respectively. Whilst $\mathbf{R}_{dq}$ matrix is diagonal, due to the mutual electro-magnetic interactions among different axes of different sets of windings within the machine, $\mathbf{L}_{dq}$ is not diagonal. Full de-coupled three-phase Field Oriented Control (FOC) can be used in multi-three phase applications transforming rotor-attached orthogonal $dq0$ reference frame variables into the Vector Space Decomposition frame (denoted with subscript vsd). The transformed nxn matrix inductance L_{vsd} is diagonal [17].

$$\mathbf{L}_{vsd} = \begin{pmatrix} d_1 & 0 & 0 & 0 & \cdots & 0 & 0 \\ 0 & q_1 & 0 & 0 & \cdots & 0 & 0 \\ 0 & 0 & d_3 & 0 & \cdots & 0 & 0 \\ 0 & 0 & 0 & q_3 & \cdots & 0 & 0 \\ \vdots & \vdots & \vdots & \vdots & \ddots & 0 & 0 \\ 0 & 0 & 0 & 0 & 0 & d_{2\nu+1} & 0 \\ 0 & 0 & 0 & 0 & 0 & 0 & q_{2\nu+1} \end{pmatrix} \tag{2}$$

In (2), $\nu = \text{trunc}((n-1)/2)$, subscripts denote harmonic orders, and d or q denotes the axis of the rotor-attached orthogonal $dq0$ reference frame.

B. Drive modelling assumptions

Distributed current control is based on previous machine modelling assumptions. Current Proportional Integral (PI) controllers are tuned on the first harmonic inductances d_1 and q_1 in (2). A simplified control diagram not considering actuation nor filtering delays is shown in Fig. 5, where Λ represents d or q axis and s is the Laplacian operator.

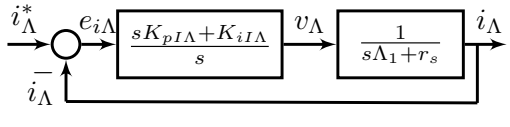

Fig. 5. Current control diagram within the synchronous reference frame without axes decoupling with first harmonic inductor Λ_1 (Λ identifies d or q axis) and the phase resistor r_s. $K_{pI\Lambda}$ and $K_{iI\Lambda}$ are the PI gains.

Once the PI controller of the simplified current loop in Fig. 5 is tuned, the closed current loop can be modelled like a low-pass filter with bandwidth ω_c and phase ϕ_c described by the following transfer function:

$$G_I = \frac{i_\Lambda}{i^*_\Lambda} = \frac{\omega_c}{s+\omega_c} = \frac{\frac{sK_{pI\Lambda}+K_{iI\Lambda}}{s}\frac{1}{s\Lambda_1+r_s}}{1+\frac{sK_{pI\Lambda}+K_{iI\Lambda}}{s}\frac{1}{s\Lambda_1+r_s}} \tag{3}$$

IV. CSR - TF COMPARISON AND DESIGN APPROACH

Both the CSR and the TF configurations are speed controlled, and as such, they both control the current with an inner control loop [20]. In nominal condition, current control within a multi-three phase motor can be achieved connecting to every set of windings one power converter commanded by its relative drive configured in torque mode. Defining the angular

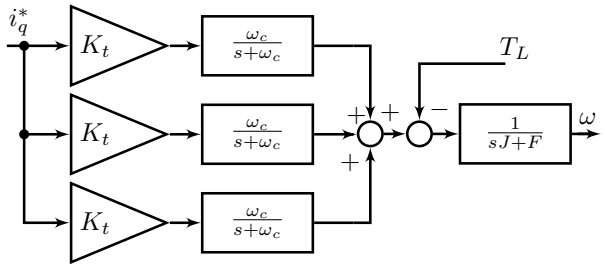

Fig. 6. Torque mode simplified diagram. Every i_q current control loop has been replaced by a low pass filter with bandwidth ω_c.

speed of the shaft ω, the machine constant K_t, the inertia J and the friction F, the simplified control diagram of the machine configured in torque mode is shown in Fig. 6. T_L is the load torque. Provided that torque and i_q current are directly proportional ($T = K_t i_q$), the final speed of the shaft at steady state depends on the balance between the i_q currents flowing within the motor and the load torque T_L [20]. The parallel of the three current loops can be further simplified with control diagram in Fig. 7. In general, speed control is set by the outer

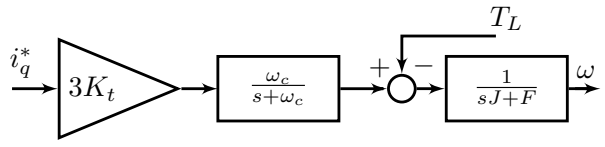

Fig. 7. Equivalent torque mode simplified diagram.

speed loop governed by a speed PI regulator. In multi-three phase application, regulators can be computed considering the loop in Fig. 8, where the equivalent (EQ) closed speed loop for

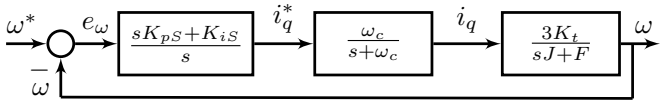

Fig. 8. Equivalent (EQ) speed control diagram. K_{pS} and K_{iS} are the PI gains.

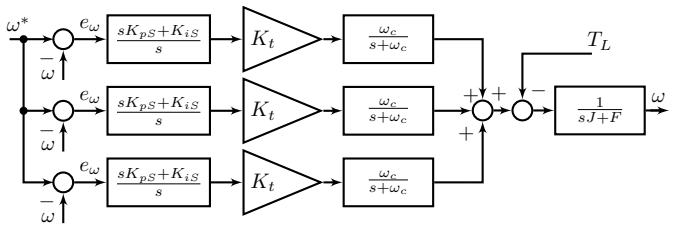

(a) Simplified common speed reference control diagram

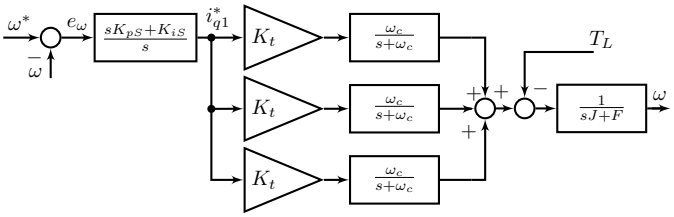

(b) Simplified torque follower control diagram (TF).

Fig. 9. Simplified common speed reference - torque follower control diagram comparison. In Fig. 9b, only the master drive on top is configured in speed mode. All the slaves are configured in torque mode and inputs are provided with the internal i_q^* current set-point from the master drive.

the CSR configuration in nominal condition is shown. Once the speed PI parameters have been computed, the same values can be used in the final simplified CSR control diagram in Fig. 9a, where there are three speed control loops in parallel.

Considering the previous discussion and assuming that both speed set-points ω^* and speed feedbacks ω are the same in every drives, the CSR and the TF simplified diagram in Fig. 9b are equivalent. In nominal condition for a given set-point, the output speeds are the same like it is shown in Fig. 10, where a speed set-point $\omega^* = 30[rad/sec]$ has been provided.

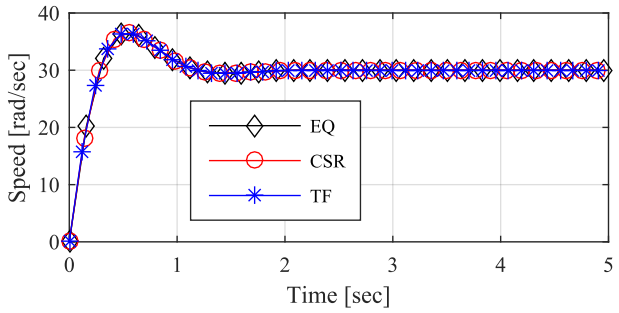

Fig. 10. Equivalence between EQ (Fig. 8), CSR (Fig. 9a) and TF (Fig. 9b) control diagram output speeds with $\omega^* = 30[rad/sec]$ and $T_L = 0[Nm]$.

The only difference is from the fault tolerance point of view. If the master drive in Fig. 9b fails, the output speed is not regulated since the follower drives are provided with the i_{q1} internal current set-point. In Fig. 11, CSR and TF output

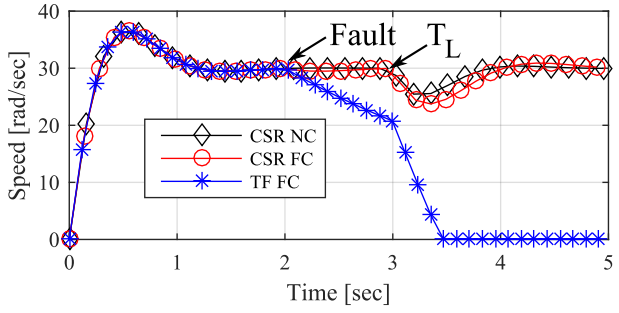

Fig. 11. TF configuration is not fault tolerant in case of master fault. After $3sec$ the load is attached and the output speed is regulated. However, CSR speed dynamic in fault condition is degraded.

speeds in Fault Condition (FC) are compared against the CSR in Nominal Condition (NC).

V. Fault Condition

Due to its distributed nature, improved fault tolerance can be achieved with the CSR configuration. However in case of fault, speed dynamics is degraded. In Fig. 11, after $3sec$ during load connection operation, lower speed dynamics in case of fault is highlighted. Assuming constant ω_c, fully fault compensation is achieved keeping constant the total gain W_T of the three paralleled loops in Fig. 9a. Defining N_A the

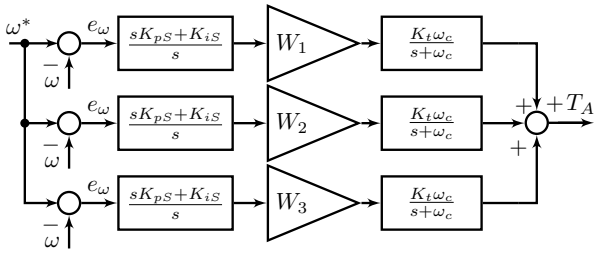

Fig. 12. $T_A = (\sum_j^{N_A} T_j)$ is the torque produced by operating modules. Speed dynamics fault compensation can be achieved updating loop gains W_j.

number of alive segments producing torque, (4) guarantees constant speed dynamics.

$$W_T = \sum_j^{N_A} W_j \tag{4}$$

For example if in nominal condition $W_1 = W_2 = W_3 = 1$, in case of open circuit fault of the third drive, the remaining two loop gains should be updated with $W_1 = W_2 = 1.5$. In Fig. 13, start-up and load step operations in nominal condition (NC), fault condition not updating (FC NU) and updating (FC U) the loop gains are shown.

VI. Case Study

Considering a real case scenario based on the rig detailed in the next section, a case study is here presented. As previously discussed in Sec. III, before tuning the current control loops the first harmonic inductances d_1 and q_1 in (2) must be obtained. Both d and q current PI gains (K_{pId}, K_{iId}, K_{pIq}, K_{iIq}) in Fig. 5 have been calculated considering a control loop bandwidth $BW_C = 211[rad/sec]$ and a phase margin $PM_C = 65°$. The speed loop regulator parameters (K_{pS}

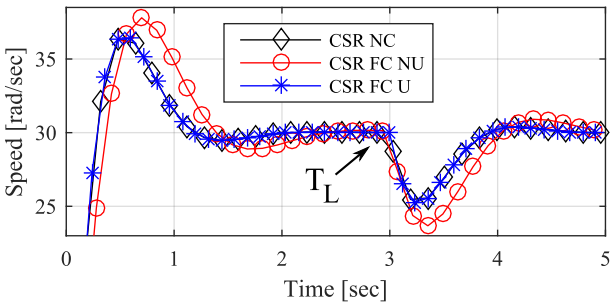

Fig. 13. In case of fault, (4) guarantees constant speed dynamics.

and K_{iS}) have been designed with a control loop bandwidth $BW_S = 6[rad/sec]$ and a phase margin $PM_S = 60°$ considering the equivalent control diagram in Fig. 8.

VII. Experimental

The equivalence between the CSR and the TF configuration as the fault compensation strategy previously discussed here are presented. As a test bench a multi-three phase two poles synchronous generator with three sets of windings shown in Fig. 14 has been used. The machine has been wired to

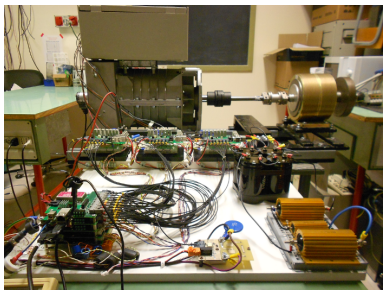

Fig. 14. Multi-three phase test rig

three off-the-shelf converters shown in the same figure. All the converters were controlled by a custom control platform named *uCube* [21]. The encoder signal has been wired to the *uCube* where three independent synchronised Field Oriented Controllers (FOC) have been coded. DC link voltage and switching frequency have been set up to $350[V]$ and $10[kHz]$, respectively. In Table I, electrical and mechanical machine parameters are reported. Speed set-point, rotor field DC current and breaking torque have been set up to $30[rad/sec]$, $1.58[A]$ and $18.36[Nm]$, respectively.

TABLE I
Machine parameters

First harmonic stator inductance $d_1[H]$	$45e^{-3}$
First harmonic stator inductance $q_1[H]$	$114e^{-3}$
Stator resistance $r_s[\Omega]$	9.1
Machine constant $K_t[Nm/A]$	3.06
Shaft inertia $J[Nms^2]$	$380e^{-3}$
Friction $F[Nms]$	$140e^{-3}$

A. CSR - TF comparison

Currents under load transient, both in CSR and TF configuration, are shown in Fig. 15. For clarity's sake, only four out eighteen currents have been highlighted. The shift of an angle $2\alpha = 2\pi/9$ between i_{a1} and i_{a3} is highlighted. Since the two configurations are equivalent and the machine

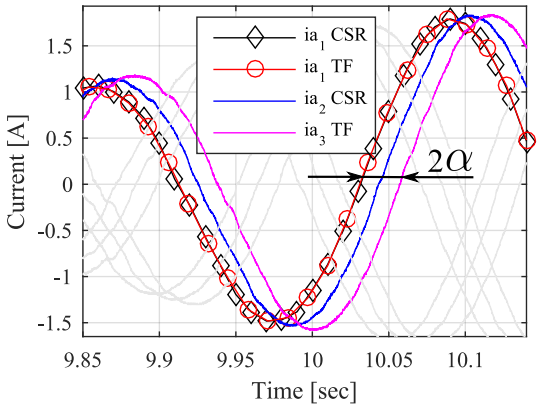

Fig. 15. Current comparison under load transient

has been started with the rotor aligned to the same position, same currents from different configurations are matching (i.e. $i_{a1}CSR$ with $i_{a1}TF$). Equivalence between the CSR and the TF configuration is further confirmed by the output speeds shown in Fig. 16.

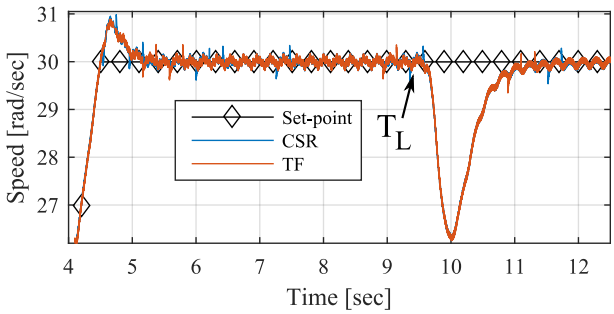

Fig. 16. During start-up and load transient operations, output speeds in CSR and TF configuration are the same.

B. Fault Compensation strategy

Disconnecting the third converter and assuming constant current bandwidth ω_c, nominal speed dynamic is guaranteed by (4). In Fig. 17, faulty output speeds updating (FC U) and not updating (FC NU) the loop gains W_j are compared against the CSR output speed in nominal condition (NC). Equation (4) guarantees constant speed operation during both start-up and load transient regulation. Assuming constant current bandwidth ω_c, elements in (2) are considered constant. In general this is not true, but in this particular case the difference is negligible. In Fig. 18, i_{q2} currents in nominal and fault conditions are shown. If in nominal condition there are $6A$ flowing within the machine - $2A$ per set -, in fault condition constant power is guaranteed with $3A$ per set.

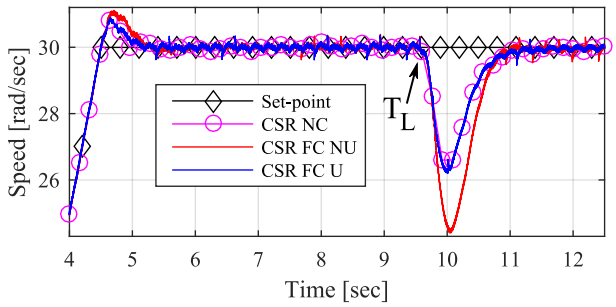

Fig. 17. In nominal condition $W_{1NC} = W_{2NC} = W_{3NC} = 1$, whilst in fault condition with updated loop gains $W_{1FC} = W_{2FC} = 1.5$.

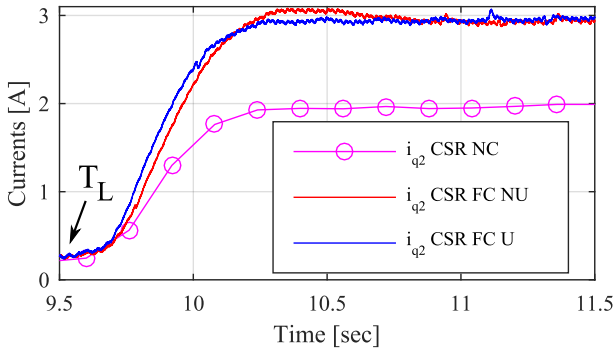

Fig. 18. Defining the total current within the motor I_T, in NC $N_A = 3$ and $I_T = (2 \cdot N_A) = 6A$, whereas in FC $N_A = 2$ and $I_T = (3 \cdot N_A) = 6A$.

VIII. Conclusion

This manuscript is focused on speed control for multi-three phase synchronous electrical motors. The equivalence between the Common Speed Reference (CSR) and the Torque Follower (TF) configuration has been demonstrated. A simplified design procedure for controlling the speed of the rotor has been analytically and experimentally validated step by step in Matlab/Simulink environment first, and then with a $22kW$ experimental rig showing good agreement with the expected results. Finally, the suggested post-fault operation in case of open-circuit condition of one three-phase set of windings has been validated. The proposed system appears to be a good candidate for some multi-three phase applications where increased reliability and fault tolerance levels are required.

References

[1] E. Levi, N. Bodo, O. Dordevic, and M. Jones, "Recent advances in power electronic converter control for multiphase drive systems," in *2013 IEEE Workshop on Electrical Machines Design, Control and Diagnosis (WEMDCD)*, March 2013, pp. 158–167.

[2] E. Levi, "Advances in converter control and innovative exploitation of additional degrees of freedom for multiphase machines," *IEEE Transactions on Industrial Electronics*, vol. 63, no. 1, pp. 433–448, Jan 2016.

[3] R. Bojoi, S. Rubino, A. Tenconi, and S. Vaschetto, "Multiphase electrical machines and drives: A viable solution for energy generation and transportation electrification," in *2016 International Conference and Exposition on Electrical and Power Engineering (EPE)*, Oct 2016, pp. 632–639.

[4] R. Abebe, G. Vakil, G. L. Calzo, T. Cox, S. Lambert, M. Johnson, C. Gerada, and B. Mecrow, "Integrated motor drives: state of the art and future trends," *IET Electric Power Applications*, vol. 10, no. 8, pp. 757–771, 2016.

[5] N. R. Brown, T. M. Jahns, and R. D. Lorenz, "Power converter design for an integrated modular motor drive," in *2007 IEEE Industry Applications Annual Meeting*, Sept 2007, pp. 1322–1328.

[6] J. Wang, Y. Li, and Y. Han, "Integrated modular motor drive design with gan power fets," *IEEE Transactions on Industry Applications*, vol. 51, no. 4, pp. 3198–3207, July 2015.

[7] M. Pulvirenti, D. D. R, N. Bianchi, G. Scarcella, and G. Scelba, "Secondary saliencies decoupling technique for self-sensing integrated multi-drives," in *2016 IEEE Symposium on Sensorless Control for Electrical Drives (SLED)*, June 2016, pp. 1–6.

[8] Y. Zhao and T. Lipo, "Space vector pwm control of dual three-phase induction machine using vector space decomposition," *Industry Applications, IEEE Transactions on*, vol. 31, no. 5, pp. 1100–1109, Sep 1995.

[9] Y. Hu, Z. Q. Zhu, and K. Liu, "Current control for dual three-phase permanent magnet synchronous motors accounting for current unbalance and harmonics," *IEEE Journal of Emerging and Selected Topics in Power Electronics*, vol. 2, no. 2, pp. 272–284, June 2014.

[10] B. Welchko, T. Lipo, T. Jahns, and S. Schulz, "Fault tolerant three-phase ac motor drive topologies: a comparison of features, cost, and limitations," *IEEE Transactions on Power Electronics*, vol. 19, no. 4, pp. 1108–1116, July 2004.

[11] A. Galassini, A. Costabeber, C. Gerada, G. Buticchi, and D. Barater, "A modular speed-drooped system for high reliability integrated modular motor drives," *IEEE Transactions on Industry Applications*, vol. 52, no. 4, pp. 3124–3132, July 2016.

[12] M. Pulvirenti, G. Scarcella, G. Scelba, M. Cacciato, and A. Testa, "Fault-tolerant ac multidrive system," *Emerging and Selected Topics in Power Electronics, IEEE Journal of*, vol. 2, no. 2, pp. 224–235, June 2014.

[13] M. A. Shamsi-Nejad, B. Nahid-Mobarakeh, S. Pierfederici, and F. Meibody-Tabar, "Fault tolerant and minimum loss control of double-star synchronous machines under open phase conditions," *IEEE Transactions on Industrial Electronics*, vol. 55, no. 5, pp. 1956–1965, May 2008.

[14] Allen-Bradley, "Load sharing applications for the 1336 impact ac drive," 1336E-WP001A-EN-P, June 2000. [Online]. Available: http://literature.rockwellautomation.com/idc/groups/literature/documents/wp/1336e-wp001_-en-p.pdf

[15] N. Mitrovic, M. Petronijevic, V. Kostic, and J. B., *Electrical Drives for Crane Application, Mechanical Engineering*, IntechOpen, Ed. M. Gokcek, 2012. [Online]. Available: http://www.intechopen.com/books/mechanical-engineering/electrical-drives-for-crane-application

[16] E. Klingshirn, "High phase order induction motors - part i-description and theoretical considerations," *IEEE Transactions on Power Apparatus and Systems,*, vol. PAS-102, no. 1, pp. 47–53, Jan 1983.

[17] A. Tessarolo, L. Branz, and M. Bortolozzi, "Stator inductance matrix diagonalization algorithms for different multi-phase winding schemes of round-rotor electric machines part i. theory," in *EUROCON 2015 - International Conference on Computer as a Tool (EUROCON), IEEE*, Sept 2015, pp. 1–6.

[18] A. Tessarolo, M. Bortolozzi, and A. Contin, "Modeling of split-phase machines in park's coordinates. part i: Theoretical foundations," in *EUROCON, 2013 IEEE*, July 2013, pp. 1308–1313.

[19] A. Galassini, A. Costabeber, M. Degano, C. Gerada, A. Tessarolo, and S. Castellan, "Distributed current control for multi-three phase synchronous machines in fault conditions," in *2016 XXII International Conference on Electrical Machines (ICEM)*, Sept 2016, pp. 1036–1042.

[20] M. P. Kazmierkowski, "Advanced electrical drives analysis, modeling, control [book news]," *IEEE Industrial Electronics Magazine*, vol. 8, no. 1, pp. 70–70, March 2014.

[21] A. Galassini, G. L. Calzo, A. Formentini, C. Gerada, P. Zancehtta, and A. Costabeber, "ucube: Control platform for power electronics," waiting for acceptance.